iScience

Article

Sex differences in the relationship between body composition and MASLD progression in a murine model of metabolic syndrome

Graphical abstract

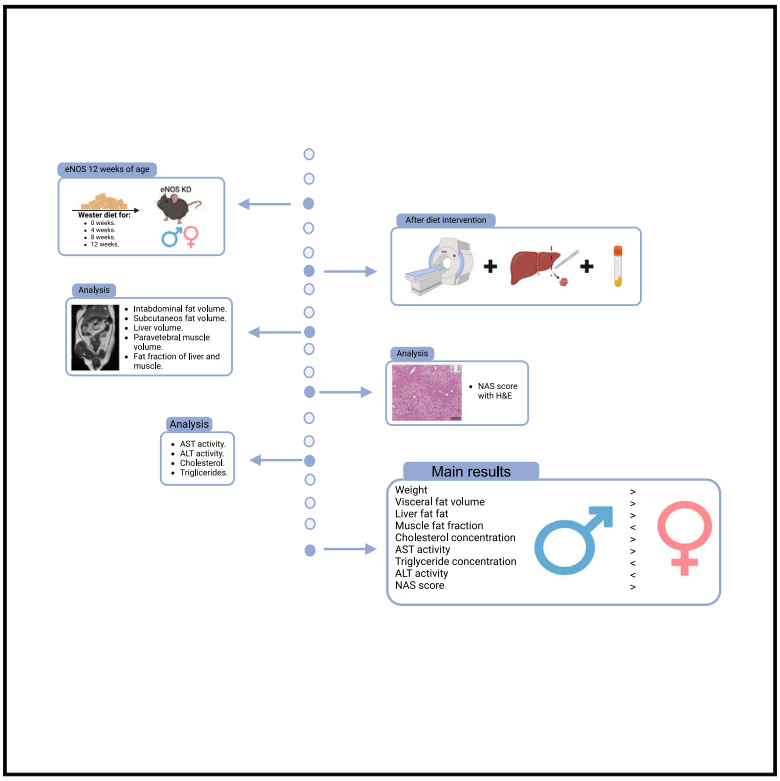

Highlights

- Body MRI reveals sex-specific patterns in body composition and MASLD progression
- Male eNOS KO mice accumulate more visceral fat and liver fat than females
- Males exhibit greater liver damage and distinct liver-to-muscle fat ratios
- Clustering analysis highlights sex-specific phenotypes of MASLD progression

Authors

Laura Manjarrés, Aline Xavier, Leticia González, ..., Alkystis Phinikaridou, Cecilia Besa, Marcelo E. Andia

Correspondence

meandia@uc.cl

In brief

Genetics; Human metabolism

Manjarrés et al., 2025, iScience *28*, 111863
February 21, 2025
https://doi.org/10.1016/j.isci.2025.111863

CellPress

iScience

CellPress
OPEN ACCESS

Article

Sex differences in the relationship between body composition and MASLD progression in a murine model of metabolic syndrome

Laura Manjarrés,[1,2] Aline Xavier,[3] Leticia González,[2,4] Camila Garrido,[2,5] Flavia C. Zacconi,[5] Katherine Rivera,[2] Laura Parra,[2] Alkystis Phinikaridou,[6] Cecilia Besa,[2,4] and Marcelo E. Andia[2,4,7,*]

[1]PhD Program in Medical Sciences, School of Medicine, Pontificia Universidad Catolica de Chile, Santiago, Chile
[2]Millennium Institute for Intelligent Healthcare Engineering, i-Health, Santiago, Chile
[3]Faculty of Engineering, Universidad de Santiago de Chile, Santiago, Chile
[4]Biomedical Imaging Center and Radiology Department, School of Medicine. Pontificia Universidad Católica de Chile, Santiago, Chile
[5]Faculty of Chemistry and Pharmacy, Pontificia Universidad Católica de Chile, Santiago, Chile
[6]School of Biomedical Engineering and Imaging Sciences, King's College London, London, UK
[7]Lead contact
*Correspondence: meandia@uc.cl
https://doi.org/10.1016/j.isci.2025.111863

SUMMARY

Metabolic dysfunction-associated steatotic liver disease (MASLD) progression exhibits significant sex differences, with males generally developing more severe disease. This study used an endothelial nitric oxide synthase knockout (eNOS KO) murine model to investigate sex-specific MASLD progression under a Western diet intervention. Magnetic resonance imaging (MRI) assessed body composition and liver and skeletal muscle fat fraction, revealing greater visceral fat, liver volume, and liver-to-muscle fat ratios in males. Dimensionality reduction and clustering analyses identified distinct sex-specific MASLD phenotypes and progression patterns. Histological evaluations confirmed greater liver damage in males, evidenced by higher MAFLD Activity Scores. These findings highlight the critical role of sex as a biological variable in MASLD pathology and emphasize the influence of body composition and fat distribution on disease progression. The study underscores the utility of advanced imaging and analytical techniques for refining non-invasive diagnostics and guiding sex-specific interventions, paving the way for personalized MASLD management strategies.

INTRODUCTION

Metabolic dysfunction-associated steatosis liver disease (MASLD), formerly known as nonalcoholic fatty liver disease (NAFLD), has emerged as a major global public health issue. Characterized as a heterogeneous disorder, MASLD involves a complex interplay of factors including age, sex, fertility status, obesity, type 2 diabetes mellitus, metabolic dysregulation, and cardiac dysfunction, among others.[1–5]

MASLD is now the most common liver disorder worldwide, with an estimated prevalence of 20%–30% among adults in developed countries, and its prevalence is rising, driven by diets high in fats and carbohydrates coupled with sedentary lifestyles.[6–8] Notably, the obesity rate currently stands at 41.5%, and approximately 69.9% of the obese population also presents with MASLD.[9,10]

While obesity has often been evaluated in patients with MASLD using general metrics such as body mass index (BMI) and waist-to-hip ratio (WHR), recent evidence suggests that fat distribution, rather than total weight, plays a more critical role in metabolic risk.[2,3,11] Specifically, the metabolic risk varies significantly between individuals with more visceral fat (often higher risk) and those with more subcutaneous fat. This distinction has led to classifications such as "metabolically healthy obese" (MHO) and "metabolically obese normal weight" (MONW). The primary difference is in fat location; MHO individuals tend to have less visceral fat than MONW individuals and are generally considered to be in a pre-disease state. Both groups, however, face higher metabolic risk than healthy individuals, albeit to varying extents.[3,11] Advanced imaging techniques can effectively differentiate between visceral and subcutaneous fat, a distinction not possible with BMI or WHR alone.[3]

Sex-based differences are also evident in MASLD, with variations in metabolic regulation, fat accumulation, genetic factors, and body fat distribution playing essential roles. For example, men typically accumulate more visceral fat due to testosterone, while premenopausal women show lower MASLD prevalence, milder fibrosis, and better survival rates, likely due to estrogen's protective effects.[2,4,12] Recent reviews highlight the substantial impact of sex hormones on fat accumulation, skeletal muscle, cardiovascular disease, and MASLD progression.[13,14]

Despite this evidence, sex-based studies in MASLD remain limited, and findings from noninvasive assessments have been

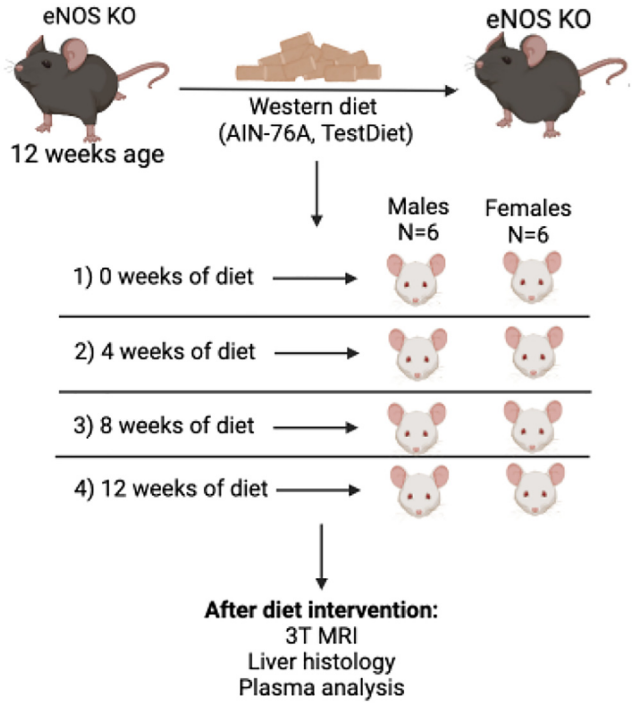

Figure 1. Study design

inconsistent.[4] Although animal models suggest sex differences, outcomes often vary based on the model used.[2,4,15,16]

Further, emerging data suggest that changes in visceral fat, subcutaneous fat, liver volume, and skeletal muscle could be predictive of disease stages; however, the role of sex in these predictive factors remains underexplored.[17]

Nitric oxide (NO) is essential in liver physiology and pathophysiology, influencing systemic functions and contributing to both hepatic and cardiovascular conditions.[18] NO derived from endothelial NO synthase (eNOS) is especially important for fat distribution, mitochondrial energy metabolism, and fatty acid regulation.[19–21]

Studies in eNOS-deficient mice show that the absence of eNOS leads to increased hepatic fat, insulin resistance, and obesity, which mirror features of metabolic syndrome in humans. These effects are further intensified under a Western diet, reflecting MASLD's progression.[18,22] In eNOS knockout (KO) mice, MASLD can be observed after 12–14 weeks on a high-calorie, high-fat diet, closely aligning with disease development seen in humans.[22]

This study aims to evaluate sex differences in body composition during MASLD progression in the double KO mice for oxide nitric synthetase (eNOS KO), using noninvasive diagnostic methods, including *in vivo* magnetic resonance imaging (MRI) and plasma analyses, complemented by histological findings.

We analyzed eight groups of eNOS KO mice (four female and four male groups, each with $n = 6$) (Figure 1). Controls consisted of eNOS KO mice maintained on a regular diet until 12 weeks of age, as previous research has established differences between eNOS KO and wild-type models.[22] When the animals were 12 weeks ± 1 week old, they were weighed and randomly assigned to a group.

RESULTS

Males have higher increase in weight than females during the diet intervention

The first weight measurement performed when the mice were assigned to a group was similar among the sex group, but not between sex.

Males gained weight throughout the whole dietary intervention, going from 26.8 ± 3.0 g in week 0 to 33.8 ± 3.9 g in week 12. Females gained weight between week 0 (19.6 ± 0.5 g) and week 8 (23.9 ± 3.0 g) reaching a plateau, and at week 12, the average weight was 23.4 ± 2.3 g.

The weight gain was higher in the first weeks of the intervention (Figure 2B). The variation of weight gain was greater in males between 0–4 weeks and 8–12 weeks; only at 4–8 weeks, females show a higher increase in weight. These weight changes occurred without showing changes in the food intake between both sexes (Figure 2C).

Males accumulate more intrabdominal fat than females

The increase in body weight was associated with an increase in the total volume of fat storage with different anatomical distribution between males and females. Males showed more total fat and visceral fat than females during the whole diet intervention, while subcutaneous fat only showed sex difference at weeks 8 and 12 (Figure 3; Table S2). When visceral fat volumes are corrected by the total fat volume and body weight, the difference by sex persists (Figures 3D and 3E).

Sex-specific differences in liver and muscle fat-fraction ratios during MAFLD progression in the eNOS mice

The liver volume increased during the diet intervention, and males showed larger livers than females at 12 weeks. Muscle loss was greater in females, showing a significant difference compared to males after 12 weeks of intervention (Figures 4A and 4C).

Paravertebral muscle fat fraction (FF) was similar in males during the whole intervention, while females exhibited an increase in the FF, which was coincident with the decrease in muscle volume. On the other hand, liver FF increased during the intervention in males, but females showed a steady behavior after the 8 weeks of diet (Figures 4B and 4D).

We analyzed the ratio between the FF of the liver and the muscle, to evaluate the different behavior between sexes. At early stages of the diet intervention, both sexes had similar ratios; however, at 8 weeks of diet, males start showing a higher ratio, and this difference get significant at 12 weeks of diet.

Plasma analysis

Total serum cholesterol was significantly higher in males during the whole intervention. On the other hand, plasma triglyceride levels were only significantly higher in males at baseline, however, when starting the intervention with the Western diet, no differences by sex were observed (Figures 5A and 5B).

Males started with higher baseline levels of aspartate aminotransferase (AST) (Figure 5C); however, during the intervention,

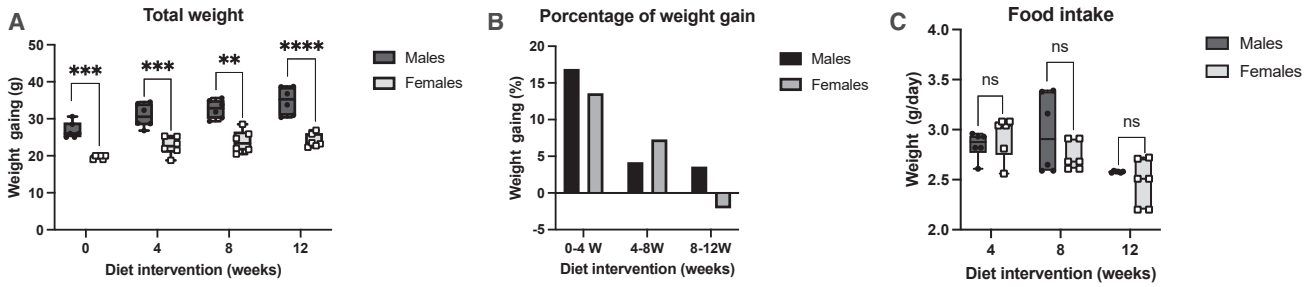

Figure 2. Weight changes during diet intervention

(A) Total weight gain during diet intervention by sex (male, black dots; female, white squares). Mann-Whitney test with min to max.

(B) Variation of weight between stages (males in black, females in gray).

(C) Food intake during diet intervention by sex (male, black dots; female, white squares). Mann-Whitney test with min, mean, and max.

ns > 0.05. *p < 0.05, **p = 0.002, ***p = 0.0006, and ****p < 0.0001.

AST progressively increased in both groups, with no significant changes between sexes. Similar trend was observed in alanine aminotransferase (ALT) activity (Figure 5D), with higher baseline levels in males and an upward trend during the intervention progression with no differences by sex. However, after 12 weeks of intervention, the female group of mice presented the highest ALT activity.

Males have a higher liver damage than females

Males had higher NAFLD Activity Score (NAS score) during the diet intervention than females, reaching a maximum NAS score of 6, while females had a maximum score of 3. Inflammation and steatosis were significantly higher in males than females during the diet intervention (Figure 6; Table S1).

Males and females showed a different relationship between liver enzyme activities and NAS score. Males showed a consistently higher NAS score than females for the same liver enzyme levels (Figure 7).

The RPCA shows a clear progression of the disease when analyzed with all the noninvasive data

A robust principal component analysis (RPCA) was performed using the non-invasive body composition data: weight, visceral fat, subcutaneous fat, total fat, liver volume, paravertebral

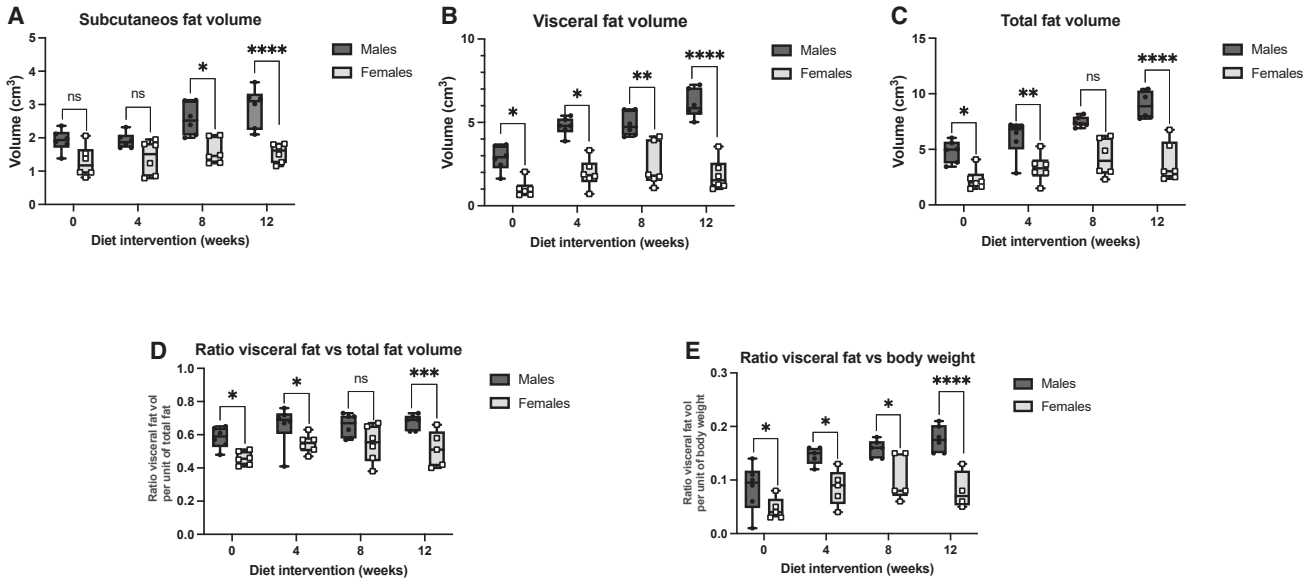

Figure 3. Fat distribution changes

(A) Differences between sex and stages in the subcutaneous fat (male, black dots; female, white squares).

(B) Differences between sex and stages in the visceral fat (male, black dots; female, white squares).

(C) Differences between sex and stages in the total fat (male, black dots; female, white squares).

(D) Differences between sex and stages in the total fat ratio per visceral fat unit (male, black dots; female, white squares).

(E) Differences between sex and stages in the visceral fat ratio per weight unit (male, black dots; female, white squares). All graphics were performed using Mann-Whitney test with min, mean, and max.

ns > 0.05. *p < 0.05, **p = 0.002, ***p = 0.0006, and ****p < 0.0001.

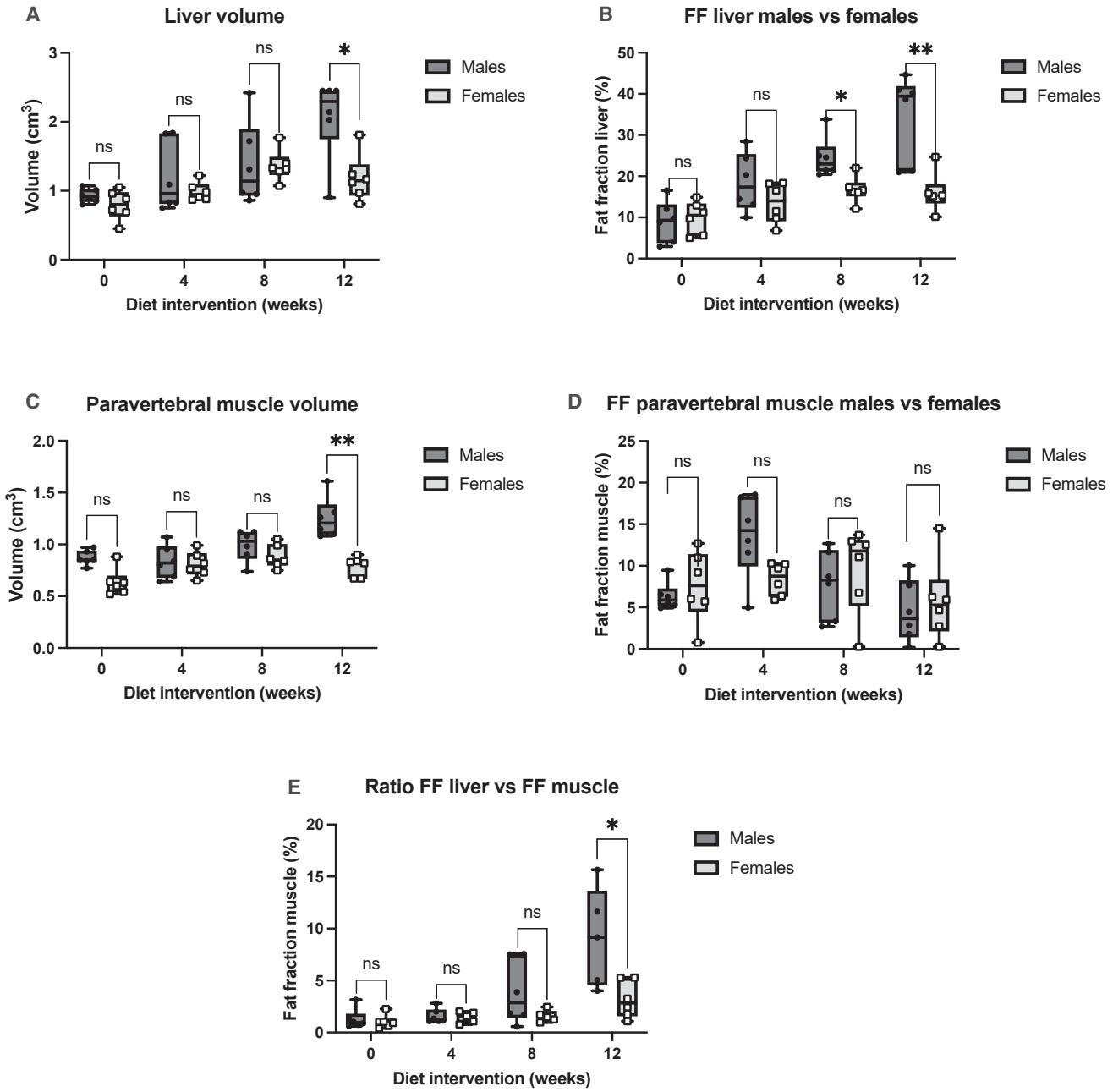

Figure 4. Fat fraction changes

(A) Differences between sex and stages in the liver volume (male, black dots; female, white squares).

(B) Differences between sex and stages in the liver FF (male, black dots; female, white squares).

(C) Differences between sex and stages in the paravertebral muscle volume (male, black dots; female, white squares).

(D) Differences between sex and stages in the paravertebral muscle volume (male, black dots; female, white squares).

(E) Differences between sex and stages in the muscle FF (male, black dots; female, white squares). All graphics were performed using Mann-Whitney test with min, mean, and max.

ns > 0.05. *$p < 0.05$ and **$p = 0.002$.

volume, FF of the liver, FF of the paravertebral muscle, ratio between visceral fat and total fat, ratio between visceral fat and weight, ratio between subcutaneous fat and weight, ratio between total fat and weight, ratio between FF liver and liver volume, ratio between FF muscle and volume muscle, and plasma analysis (AST activity, ALT activity, cholesterol concentration, and triglyceride concentration). Figure 8A showed the robust principal components 1 and 2 and the K-nearest neighbors

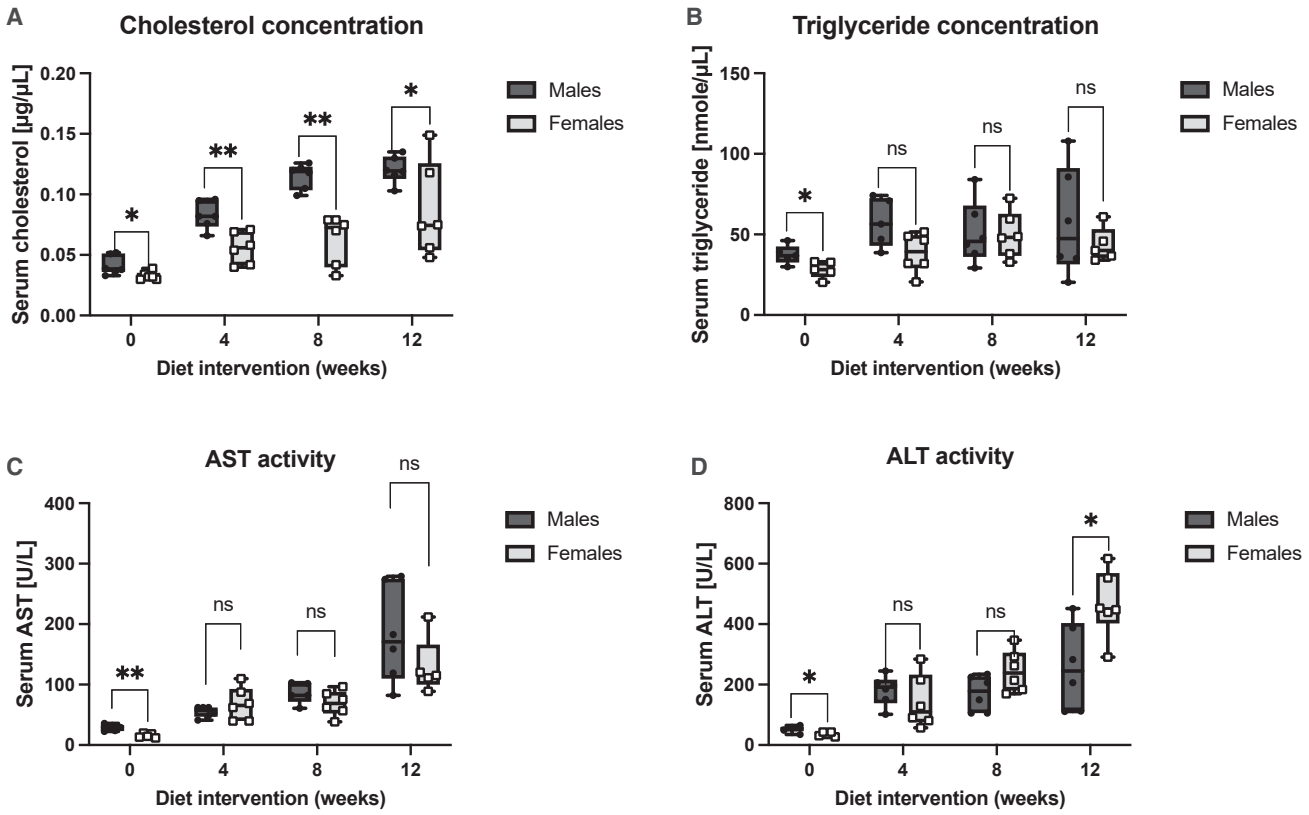

Figure 5. Plasma analysis

(A) Differences between sex and stages in cholesterol concentration in µg/µL (male, black dots; female, white squares).

(B) Differences between sex and stages in triglyceride concentration in nmol/µL (male, black dots; female, white squares).

(C) Differences between sex and stages in the AST activity in U/L (male, black dots; female, white squares).

(D) Differences between sex and stages in the ALT activity in U/L (male, black dots; female, white squares). All graphics were performed using Mann-Whitney test with min, mean, and max.

ns > 0.05. *p < 0.05, **p = 0.002, ***p = 0.0006, and ****p < 0.0001.

analysis clusters of the male-only data showing a clear separation between different stage of liver disease progression. Figure 8B showed the same analysis in female-only data, showing also a clear separation of the disease's progression. However, when male and female data were analyzed together (Figure 8C), the classification showed a very low performance, suggesting that the analysis of the disease progression is better interpreted when performed separately by sex.

We compared the clusters obtained in the RPCA with the NAS score (Figure 9); in the graphics, we saw that the clusters can predict very well the NAS score, especially in males.

DISCUSSION

This study provides new evidence on sex-specific differences in MASLD progression in an eNOS KO mouse model, highlighting the complex interplay between body composition and liver pathology over time. Males showed higher amounts of intra-abdominal fat, triglyceride levels, and higher AST activity; these noninvasive findings were related to a higher histological liver damage score (NAS score). Furthermore, the multidimensional analysis of noninvasive data on body composition and serological markers of circulating liver enzymes and lipids, separated by sex, allowed to distinguish the different stages of MASLD progression, opening an opportunity to improve noninvasive diagnosis and follow-up.

Our findings are consistent with previous studies that underscore the importance of sex and fat distribution in metabolic diseases.[3,11,17,23] However, by utilizing the eNOS KO model fed with Western diet, under a house temperature of 22°C, this study uniquely reveals how these factors manifest differently between males and females in MASLD.

Males exhibited greater liver fat accumulation, visceral fat, and more pronounced liver damage, as reflected by higher NAS scores. These observations align with epidemiological data showing that males generally experience faster MASLD progression than females.[24,25] This difference has been attributed to the protective role of estrogen in females, which helps mitigate hepatic fibrosis and inflammation during earlier disease stages.[13,23] Our data suggest that females store a proportionally greater proportion of fat in skeletal muscle than in the liver compared to males. This finding is consistent with the concept

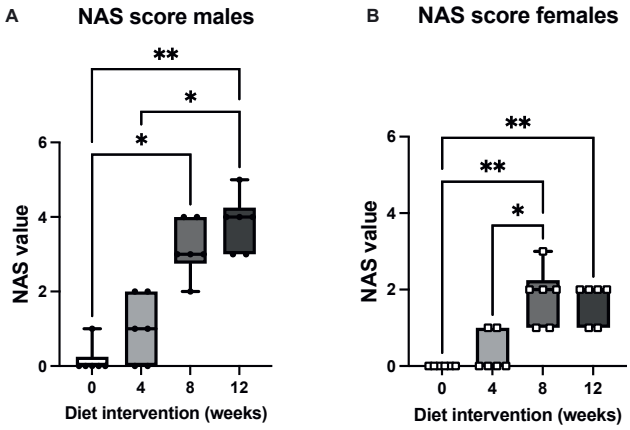

Figure 6. NAS score per animal during the diet intervention

(A) Females.

(B) Males. All graphics were performed using Kruskal-Wallis test with min, mean, and max.

ns > 0.05. *$p < 0.05$, **$p = 0.002$, ***$p = 0.0006$, and ****$p < 0.0001$.

of skeletal muscle acting as a metabolic buffer, which has been proposed in other studies.[26] In contrast, males consistently exhibited higher liver fat-to-muscle FFs, indicating a lack of such metabolic protection and an increased susceptibility to liver damage. Recent research supports this phenomenon, noting that muscle mass preservation can significantly reduce the burden of liver fat accumulation and may protect against advanced liver disease.[3,23]

Our unsupervised data analysis followed by the clustering algorithm further revealed that disease progression and clustering differed markedly by sex. These results highlight the necessity of incorporating sex-specific approaches when evaluating MASLD progression, as evidenced by other reviews recommending sex-based stratification in metabolic disease diagnostics and treatment.[13,23]

Another critical contribution of our study is the use of noninvasive imaging methods, specifically body composition MRI, to not only predict the MASLD staging, as other studies have suggested,[17] but also the images could provide a dynamic, less invasive alternative to traditional biopsy, especially valuable in early-stage diagnosis and patient follow-up.

Overall, our findings suggest that body composition, particularly muscle-fat interaction, plays a crucial role in delaying liver damage in females. This aligns with studies emphasizing estrogen's influence on fat distribution and inflammation reduction, though our study indicates that prolonged Western diet exposure may attenuate this effect.[17,27] Moving forward, research should examine how hormonal transitions, especially menopause, may impact these protective mechanisms and assess the role of skeletal muscle and fat in different MASLD stages.

Conclusion

In conclusion, this study confirms that MASLD progression in response to a Western diet differs significantly between sexes in the eNOS KO model, with body composition changes closely linked to liver damage. By differentiating MASLD progression by sex, our results provide a more nuanced understanding of disease pathology, suggesting that muscle fat dynamics are integral to sex-specific outcomes. These results are consistent with literature that underscores the role of sex hormones, particularly estrogen, in mediating metabolic diseases.[13,27] Future studies should delve further into sex differences, examining hormonal shifts, gut-liver axis interactions, and organ-specific impacts in MASLD, particularly involving muscle, heart, and brain.[14,27,28]

Limitations of the study

The primary limitation of this study is the use of an eNOS KO murine model, which, while faithfully mimicking many aspects of human MASLD progression, requires validation in human populations to confirm its clinical relevance. Additionally, the 12-week diet intervention was insufficient to observe significant liver fibrosis, limiting insights into sex-specific differences in advanced disease stages. Finally, the small volume of plasma available per mouse constrained the scope of biochemical analyses. Future studies should extend intervention durations and expand plasma analyses to provide a more comprehensive understanding of MASLD progression and its sex-specific characteristics.

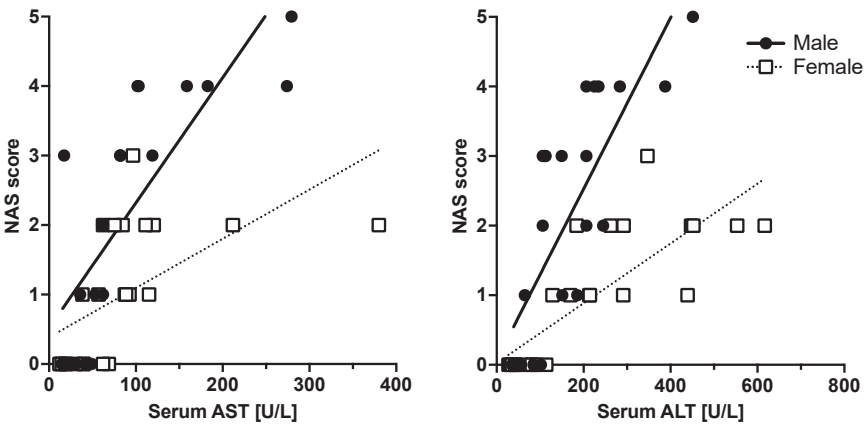

Figure 7. NAS score versus AST and ALT activity

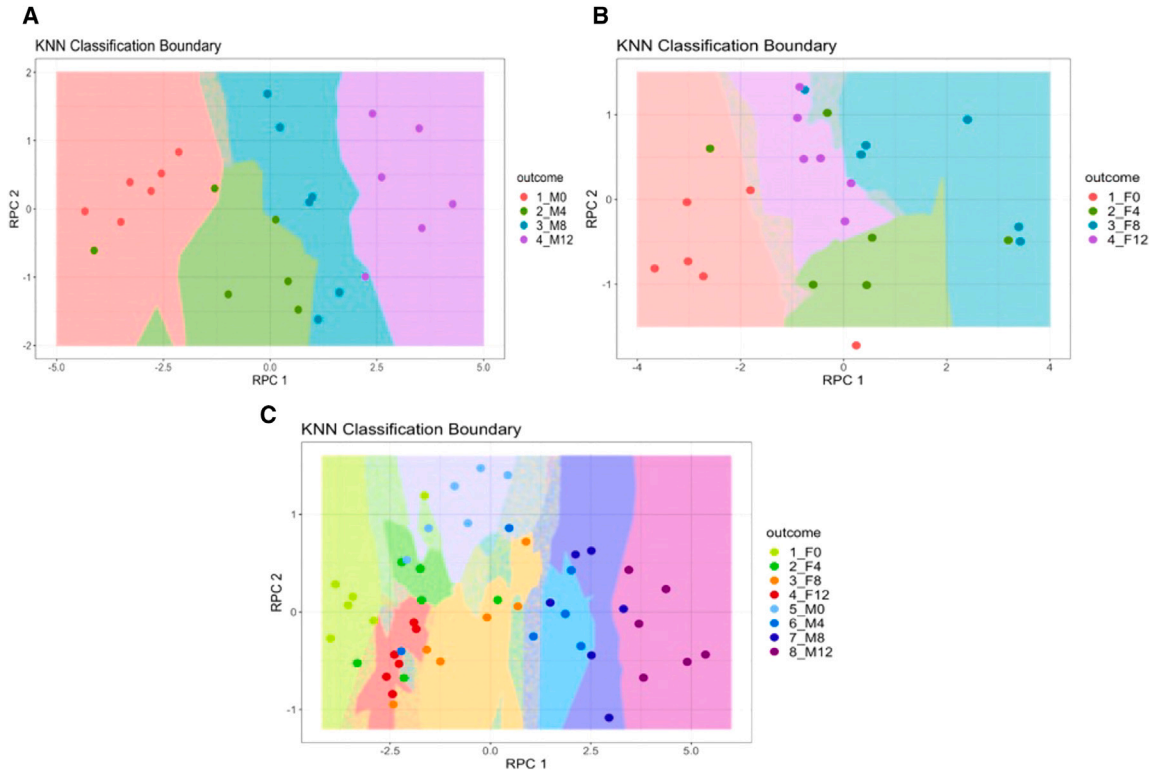

Figure 8. RPCA analysis and KNN classification

(A) KNN for males, in red is the cluster for the control group, in red is the cluster for the 4-week diet group, in purple is the cluster for the 8-week diet group, and in green is the cluster for the 12-week diet group.

(B) KNN for females, in red is the cluster for the control group, in red is the cluster for the 4-week diet group, in purple is the cluster for the 8-week diet group, and in green is the cluster for the 12-week diet group.

(C) KNN for all animals, in light green is the cluster for the female control group, in light blue is the cluster for the male control group, in dark green is the cluster for the female 4-week diet group, in blue is the cluster for the male 4-week diet group, in orange is the cluster for the female 8-week diet group, in dark blue is the cluster for the male 8-week diet group, in red is the cluster for the female 12-week diet group, and in purple is the cluster for the male 12-week diet group.

RESOURCE AVAILABILITY

Lead contact

Requests for further information and resources should be directed to and will be fulfilled by the lead contact, Marcelo E. Andia (meandia@uc.cl).

Materials availability

This study did not generate new unique reagents.

Data and code availability

All data reported in this paper will be shared by the lead contact upon request.

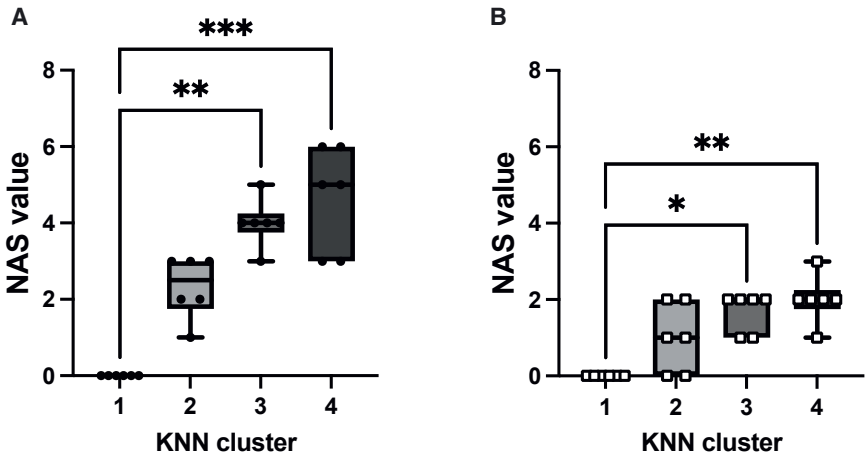

Figure 9. NAS score in the RPCA clusters

(A) Males.

(B) Females. All graphics were performed using Kruskal-Wallis test with min to max.

ns > 0.05. *$p < 0.05$, **$p = 0.002$, ***$p = 0.0006$, and ****$p < 0.0001$.

ACKNOWLEDGMENTS

This work was partially funded by ANID – Millennium Science Initiative Program – ICN2021_004 and FONDECYT 1220922, Chilean Agency for Research and Development (ANID).

AUTHOR CONTRIBUTIONS

L.M., A.X., C.B., and M.E.A. designed the experiments, analyzed the data, and prepared the manuscript. L.M. wrote the first draft. L.M., L.G., K.R., L.P., and C.G. supervised the animal model. L.M., A.X., C.B., F.C.Z., A.P., and M.E.A. performed MRI imaging and spectroscopy acquisition and analysis. L.M., A.X., C.G., A.P., and M.E.A. conducted histology and serum analysis.

DECLARATION OF INTERESTS

The authors declare no competing interests.

STAR★METHODS

Detailed methods are provided in the online version of this paper and include the following:

- KEY RESOURCES TABLE
- EXPERIMENTAL MODEL AND STUDY PARTICIPANT DETAILS
  - Animal model
  - Ethics Statement
- METHOD DETAILS
  - Diet intervention
  - MRI imaging
  - Histology
  - Cholesterol assay
  - Triglyceride assay
  - ALT assay
  - AST assay
- QUANTIFICATION AND STATISTICAL ANALYSIS
  - Data analysis
  - Body composition analysis
  - Principal component analysis

SUPPLEMENTAL INFORMATION

Supplemental information can be found online at https://doi.org/10.1016/j.isci.2025.111863.

Received: September 2, 2024
Revised: November 30, 2024
Accepted: January 3, 2025
Published: January 20, 2025

REFERENCES

1. Xavier, A., Zacconi, F., Santana-Romo, F., Eykyn, T.R., Lavin, B., Phinikaridou, A., Botnar, R., Uribe, S., Oyarzún, J.E., Cabrera, D., et al. (2021). Assessment of hepatic fatty acids during non-alcoholic steatohepatitis progression using magnetic resonance spectroscopy. Ann. Hepatol. *25*, 1000570. https://linkinghub.elsevier.com/retrieve/pii/S1665268121000570.
2. Eslam, M., Sanyal, A.J., George, J., International Consensus Panel; Neuschwander-Tetri, B., and Tiribelli, C. (2020). MAFLD: A Consensus-Driven Proposed Nomenclature for Metabolic Associated Fatty Liver Disease. Gastroenterology *158*, 1999–2014.e1. https://linkinghub.elsevier.com/retrieve/pii/S0016508520301712.
3. Després, J.P. (2012). Body Fat Distribution and Risk of Cardiovascular Disease: An Update. Circulation *126*, 1301–1313. https://doi.org/10.1161/CIRCULATIONAHA.111.067264.
4. Lonardo, A., Nascimbeni, F., Ballestri, S., Fairweather, D., Win, S., Than, T.A., Abdelmalek, M.F., and Suzuki, A. (2019). Sex Differences in Nonalcoholic Fatty Liver Disease: State of the Art and Identification of Research Gaps. Hepatology *70*, 1457–1469. https://doi.org/10.1002/hep.30626.
5. Loomba, R., Friedman, S.L., and Shulman, G.I. (2021). Mechanisms and disease consequences of nonalcoholic fatty liver disease. Cell *184*, 2537–2564. https://linkinghub.elsevier.com/retrieve/pii/S0092867421004943.
6. Rinella, M.E., Neuschwander-Tetri, B.A., Siddiqui, M.S., Abdelmalek, M.F., Caldwell, S., Barb, D., Kleiner, D.E., and Loomba, R. (2023). AASLD Practice Guidance on the clinical assessment and management of nonalcoholic fatty liver disease. Hepatology *77*, 1797–1835. https://doi.org/10.1097/HEP.0000000000000323.
7. Brouwers, M.C.G.J., Simons, N., Stehouwer, C.D.A., and Isaacs, A. (2020). Non-alcoholic fatty liver disease and cardiovascular disease: assessing the evidence for causality. Diabetologia *63*, 253–260. https://doi.org/10.1007/s00125-019-05024-3.
8. Brouwers, M.C.G.J., Simons, N., Stehouwer, C.D.A., and Isaacs, A. (2020). Non-alcoholic fatty liver disease and cardiovascular disease: assessing the evidence for causality. Diabetologia *63*, 253–260.
9. Wong, M.C.S., Huang, J., Wang, J., Chan, P.S.F., Lok, V., Chen, X., Leung, C., Wang, H.H.X., Lao, X.Q., and Zheng, Z.J. (2020). Global, regional and time-trend prevalence of central obesity: a systematic review and meta-analysis of 13.2 million subjects. Eur. J. Epidemiol. *35*, 673–683. https://doi.org/10.1007/s10654-020-00650-3.
10. Quek, J., Chan, K.E., Wong, Z.Y., Tan, C., Tan, B., Lim, W.H., Tan, D.J.H., Tang, A.S.P., Tay, P., Xiao, J., et al. (2023). Global prevalence of non-alcoholic fatty liver disease and non-alcoholic steatohepatitis in the overweight and obese population: a systematic review and meta-analysis. Lancet. Gastroenterol. Hepatol. *8*, 20–30. https://linkinghub.elsevier.com/retrieve/pii/S246812532200317X.
11. Loos, R.J.F., and Kilpeläinen, T.O. (2018). Genes that make you fat, but keep you healthy. J. Intern. Med. *284*, 450–463.
12. Yang, J.D., Abdelmalek, M.F., Pang, H., Guy, C.D., Smith, A.D., Diehl, A.M., and Suzuki, A. (2014). Gender and menopause impact severity of fibrosis among patients with nonalcoholic steatohepatitis. Hepatology *59*, 1406–1414. https://doi.org/10.1002/hep.26761.
13. Cherubini, A., Della Torre, S., Pelusi, S., and Valenti, L. (2024). Sexual dimorphism of metabolic dysfunction-associated steatotic liver disease. Trends Mol. Med. *30*, 1126–1136. https://linkinghub.elsevier.com/retrieve/pii/S1471491424001357.
14. Wang, J., and Lonardo, A. (2023). Commentary: Of women, liver, and heart. Metab. Target Organ Damage *3*, 14. https://www.oaepublish.com/articles/mtod.2023.23.
15. Yasuda, M., Shimizu, I., Shiba, M., and Ito, S. (1999). Suppressive effects of estradiol on dimethylnitrosamine-induced fibrosis of the liver in rats. Hepatology *29*, 719–727. https://doi.org/10.1002/hep.510290307.
16. Cvitanović Tomaš, T., Urlep, Ž., Moškon, M., Mraz, M., and Rozman, D. (2018). Liver sex Computational Model: Sexual Aspects in Hepatic Metabolism and Abnormalities. Front Physiol. *9*, 360. https://doi.org/10.3389/fphys.2018.00360.
17. Mahmoud, O.M., Mahmoud, G.A.E., Atta, H., Abbas, W.A., Ahmed, H.M., and Abozaid, M.A.A. (2023). Visceral and subcutaneous fat, muscle mass, and liver volume as noninvasive predictors of the progress of non-alcoholic fatty liver disease. Egypt. J. Radiol. Nucl. Med. *54*, 5. https://doi.org/10.1186/s43055-022-00949-z.
18. Iwakiri, Y., and Kim, M.Y. (2015). Nitric oxide in liver diseases. Trends Pharmacol. Sci. *36*, 524–536. https://linkinghub.elsevier.com/retrieve/pii/S0165614715000917.
19. Nozaki, Y., Fujita, K., Wada, K., Yoneda, M., Shinohara, Y., Imajo, K., Ogawa, Y., Kessoku, T., Nakamuta, M., Saito, S., et al. (2015). Deficiency of eNOS exacerbates early-stage NAFLD pathogenesis by changing the fat distribution. BMC. Gastroenterol. *15*, 177. https://doi.org/10.1186/s12876-015-0409-9.

20. Doulias, P.T., Tenopoulou, M., Greene, J.L., Raju, K., and Ischiropoulos, H. (2013). Nitric Oxide Regulates Mitochondrial Fatty Acid Metabolism Through Reversible Protein *S* -Nitrosylation. Sci. Signal. *6*, rs1. https://doi.org/10.1126/scisignal.2003252.

21. Gouill, E.L., Jimenez, M., Binnert, C., Jayet, P.Y., Thalmann, S., Nicod, P., Scherrer, U., and Vollenweider, P. (2007). Endothelial Nitric Oxide Synthase (eNOS) Knockout Mice Have Defective Mitochondrial β-Oxidation. Diabetes *56*, 2690. https://diabetesjournals.org/diabetes/article/56/11/2690/13620/Endothelial-Nitric-Oxide-Synthase-eNOS-Knockout.

22. Lavin, B., Eykyn, T.R., Phinikaridou, A., Xavier, A., Kumar, S., Buqué, X., Aspichueta, P., Sing-Long, C., Arrese, M., Botnar, R.M., and Andia, M.E. (2023). Characterization of hepatic fatty acids using magnetic resonance spectroscopy for the assessment of treatment response to metformin in an eNOS$^{-/-}$ mouse model of metabolic nonalcoholic fatty liver disease/nonalcoholic steatohepatitis. NMR Biomed. *36*, e4932. https://doi.org/10.1002/nbm.4932.

23. Schorr, M., Dichtel, L.E., Gerweck, A.V., Valera, R.D., Torriani, M., Miller, K.K., and Bredella, M.A. (2018). Sex differences in body composition and association with cardiometabolic risk. Biol. Sex Differ. *9*, 28. https://doi.org/10.1186/s13293-018-0189-3.

24. Srikanthan, P., Horwich, T.B., Calfon Press, M., Gornbein, J., and Watson, K.E. (2021). Sex Differences in the Association of Body Composition and Cardiovascular Mortality. J. Acad. Hosp. Adm. *10*, e017511. https://doi.org/10.1161/JAHA.120.017511.

25. Pradhan, A.D. (2014). Sex Differences in the Metabolic Syndrome: Implications for Cardiovascular Health in Women. Clin. Chem. *60*, 44–52. https://academic.oup.com/clinchem/article/60/1/44/5581485.

26. Yi, X., Li, W., Wang, G., Li, P., Sun, X., Tang, H., Cui, B., Ling, J., Luo, P., Fu, Z., et al. (2023). Sex-Specific Changes in Body Composition Following Metabolic and Bariatric Surgery Are Associated with the Remission of Metabolic Syndrome. Obes. Surg. *33*, 2780–2788. https://doi.org/10.1007/s11695-023-06741-w.

27. Bellissimo, M.P., Fleischer, C.C., Reiter, D.A., Goss, A.M., Zhou, L., Smith, M.R., Kohlmeier, J., Tirouvanziam, R., Tran, P.H., Hao, L., et al. (2022). Sex differences in the relationships between body composition, fat distribution, and mitochondrial energy metabolism: a pilot study. Nutr. Metab. *19*, 37. https://doi.org/10.1186/s12986-022-00670-8.

28. Hartman, H.S., Kim, E., Carbone, S., Miles, C.H., and Reilly, M.P. (2024). Sex differences in the relationship between body composition and cardiac structure and function. Eur. Heart J. Cardiovasc. Imaging, jeae264. https://doi.org/10.1093/ehjci/jeae264/7820633.

STAR★METHODS

KEY RESOURCES TABLE

REAGENT or RESOURCE	SOURCE	IDENTIFIER
Experimental models: Organisms/strains		
eNOS KO Mice	Animal Facility, Pontifica Universidad Católica de Chile	Jackson Laboratory, Strain #:002684
Other		
Chow Diet	TestDiet	5P00
Western Diet	TestDiet	AIN-76A
Chemicals, peptides, and recombinant proteins		
Xylazine	Sigma-Aldrich	Cat# X1251
Ketamine	Sigma-Aldrich	Cat# K2753
Formalin	Sigma-Aldrich	Cat# HT5011
Critical commercial assays		
Cholesterol Assay Kit	Sigma-Aldrich	Cat# MAK043
Triglyceride Assay kit	Sigma-Aldrich	Cat# MAK266
ALT	Human	Cat# 12212
AST	Human	Cat# 12211
Software and algorithms		
MRI Scanner	Philips	Ingenia 3T
Horos Software	horosproject.org	Version 3.3.6
GraphPad Prism	GraphPad Soft	Version 9
R Statistical Software	www.r-project.org/	Version 4.0.2

EXPERIMENTAL MODEL AND STUDY PARTICIPANT DETAILS

Animal model

Male and female eNOS KO mice (12 weeks old) were used to study MAFLD progression. The model mimics the metabolic syndrome observed in humans. Mice were maintained under controlled conditions (12-hour light/dark cycle, Temperature: 22±1°C) with free access to food and water.

Animals were supervised daily following institutional guidelines; and food intake and body weight were controlled by weighing them on a scale (±1g) and recorded throughout the study. All procedures were performed following recommendations from the Guide for the Care and Use of Laboratory Animals published by the US National Institutes of Health and were approved by the Ethics and Animal Welfare Committee from Pontificia Universidad Católica de Chile.

Ethics Statement

All procedures were approved by the Ethics and Animal Welfare Committee of Pontificia Universidad Católica de Chile (ID 210617015) and complied with the Guide for the Care and Use of Laboratory Animals.

METHOD DETAILS

Diet intervention

Mice were randomized into four groups per sex and fed a Western diet (4.49 kcal/g; 40% fat, 15.8% protein, 44.2% carbohydrate) for 0, 4, 8, or 12 weeks. Each group had similar weight at the begging.

MRI imaging

After the diet intervention, 3T MRI scans were performed using a Philips Ingenia scanner to assess body composition and fat-fraction. Parameters included T1-weighted images for liver visualization and two-point Dixon sequences for fat-fraction analysis.

Histology

Liver samples were fixed in 10% formalin, embedded in paraffin, sectioned (3μm), and stained with hematoxylin and eosin (H&E). A blinded pathologist assessed liver damage using the NAFLD Activity Score (NAS).

Cholesterol assay

Plasma cholesterol was measured using a colorimetric assay, and absorbance was recorded at 570 nm.

Triglyceride assay

Plasma triglycerides was measured using a colorimetric assay, and absorbance was recorded at 570 nm.

ALT assay

ALT was measured by adapting a human kit for enzyme analysis. The enzyme activity was evaluated by reading the activity 1 time per minute for 5 minutes with a wavelength of 365nm.

AST assay

AST was measured by adapting a human kit for enzyme analysis. The enzyme activity was evaluated by reading the activity 1 time per minute for 5 minutes with a wavelength of 365nm.

QUANTIFICATION AND STATISTICAL ANALYSIS

Data analysis

Statistical analyses were conducted using Prism 9 (GraphPad Software) and R version 4.0.2. Normality of data distribution was assessed using the Shapiro–Wilk test. Depending on the data distribution, the Kruskal–Wallis test or Mann–Whitney U test was applied to compare groups, with a significance threshold of $P < 0.05$.

For multivariate analyses, robust principal component analysis (RPCA) and K-nearest neighbors (KNN) clustering were applied to raw data. Cluster validation was based on visual separation in RPCA plots and agreement with known.

All analyses used a sample size of n = 6 animals per group. Data are represented as mean ± standard error of the mean (SEM) in all figures, with exact details provided in figure legends and the results section. Outliers were identified and excluded using tests available in Prism.

Boxplots, bar graphs, and other visual data representations show the mean as the center line, with whiskers indicating SEM. Detailed statistical information, including P-values, measures of center and dispersion, and exact statistical tests, can be found in the corresponding figure legends and results section.

Body composition analysis

MRI data were analyzed using Horos software. Parameters like total, visceral, and subcutaneous fat were manually segmented.

Principal component analysis

Robust PCA (RPCA) was applied to MRI and cholesterol data to determine disease clustering, using R libraries (rpca, class, caret).